

Communication

**A solid-solution approach for redox active metal
 organic frameworks with tunable redox conductivity**

Gavin S. Mohammad-Pour, Kendrich O. Hatfield, David C. Fairchild, Kenneth Hernandez-Burgos, Joaquín Rodríguez-López, and Fernando J. Uribe-Romo

J. Am. Chem. Soc., **Just Accepted Manuscript** • Publication Date (Web): 01 Dec 2019

Downloaded from pubs.acs.org on December 2, 2019

Just Accepted

“Just Accepted” manuscripts have been peer-reviewed and accepted for publication. They are posted online prior to technical editing, formatting for publication and author proofing. The American Chemical Society provides “Just Accepted” as a service to the research community to expedite the dissemination of scientific material as soon as possible after acceptance. “Just Accepted” manuscripts appear in full in PDF format accompanied by an HTML abstract. “Just Accepted” manuscripts have been fully peer reviewed, but should not be considered the official version of record. They are citable by the Digital Object Identifier (DOI®). “Just Accepted” is an optional service offered to authors. Therefore, the “Just Accepted” Web site may not include all articles that will be published in the journal. After a manuscript is technically edited and formatted, it will be removed from the “Just Accepted” Web site and published as an ASAP article. Note that technical editing may introduce minor changes to the manuscript text and/or graphics which could affect content, and all legal disclaimers and ethical guidelines that apply to the journal pertain. ACS cannot be held responsible for errors or consequences arising from the use of information contained in these “Just Accepted” manuscripts.

A solid-solution approach for redox active metal organic frameworks with tunable redox conductivity

Gavin S. Mohammad-Pour,¹† Kendrick O. Hatfield,²‡ David C. Fairchild,¹ Kenneth Hernandez-Burgos,² Joaquín Rodríguez-López,^{2,*} and Fernando J. Uribe-Romo^{1,*}

¹Department of Chemistry, University of Central Florida, Orlando, FL 32816-2366, USA.

²Department of Chemistry and Beckman Institute for Advanced Science and Technology, University of Illinois at Urbana–Champaign, Urbana, Illinois 61820, USA.

Supporting Information Placeholder

ABSTRACT:

Systematically tuning the conductivity of metal-organic frameworks (MOFs) is key to synergizing their attractive synthetic control and porosity with electrochemical attributes useful in energy and sensing technologies. *A priori* control of charge transfer is possible by exploiting the solid-solution properties of MOFs together with electronic self-exchange enabled by redox pendants. Here we introduce a new strategy for preparing redox-active MOF thin film electrodes with finely tuned redox pendant content. Varying the ratios of alkyl-ferrocene containing redox-active and inactive links during MOF synthesis enabled the fabrication of electrodes with tunable redox conductivity. The prepared MOF electrodes display maximum electron conductivity of 1.10 mS m^{-1} , with crystallographic and electrochemical stability upon thousands of redox cycles. Electroanalytical studies demonstrated that the conductivity follows solution-like diffusion-controlled behavior with non-linear electron diffusion coefficients consistent with charge-hopping and percolation models of spatially fixed redox centers. Our studies create new prospects in the design and synthesis of redox-active MOFs with targeted properties for the design of advanced electrochemical devices.

Understanding charge transport in reticular materials like metal-organic frameworks (MOFs) creates opportunities for advanced device design in photovoltaics,¹⁻³ energy storage,^{4,7} electrocatalysts,⁸⁻¹⁰ and electrochemical sensors.¹¹⁻¹⁴ Of the many strategies proposed to impose conductivity in MOFs, covalent incorporation of redox active mediators (RAMs) into otherwise dielectric MOFs¹⁵⁻²² offers the advantage of high modularity via synthesis, enabling systematic composition-property relationship studies. This strategy takes advantage of a diversity of available RAMs which display wide ranges of redox potentials and electron transfer kinetics.²³⁻²⁶ In this manner, charge transport in MOFs through the use of attached RAMs is attributed to electron “hopping” mediated by self-exchange reactions that result in diffusion of electrons within the MOF, creating an electric current. By incorporating RAMs with known fast self-exchange kinetics, it is possible to predesign MOFs that exhibit high redox-based conductivity. Several strategies have been explored to incorporate RAMs into MOFs, such as: non-covalent impregnation of guest RAMs in the pores,^{15, 17} using RAMs in single-linker MOFs,⁹ and via post-synthetic covalent tethering of RAMs at the defect sites of the MOF.^{16, 18-20, 22} Going forward, it is desirable to access a versatile synthetic platform that enables homogeneous and systematic modification of redox loading while preserving MOF structure. In this

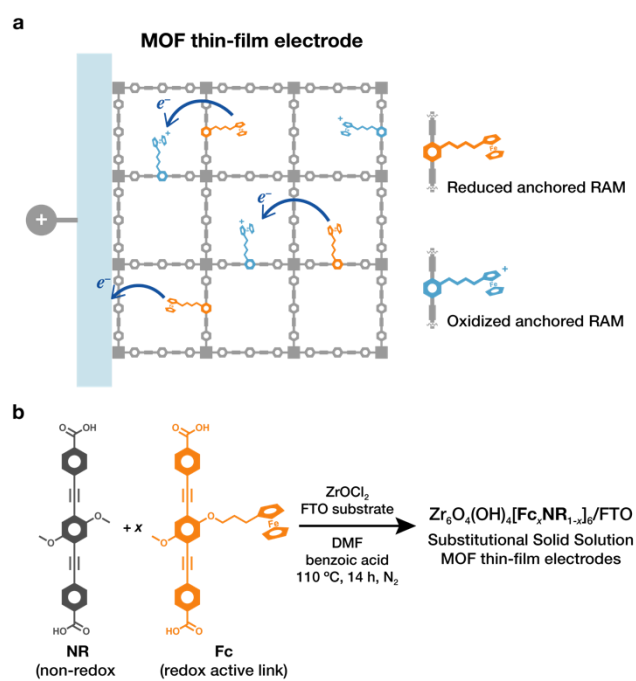


Figure 1. (a) Depiction of a MOF thin film electrode containing varied amounts of redox active links that enable fast redox conductivity via redox hopping. (b) Synthesis of MOF thin film electrodes with finely tunes substitutional solid solution amounts of redox active links.

communication, we present a new strategy for tuning the redox conductivity of multivariate MOFs²⁷ using the concept of substitutional solid solutions (SSS),²⁸ by incorporating varied amounts of links containing covalently bound RAMs that display fast electron exchange kinetics (Figure 1a). For this purpose, we anchored ω -alkyl-ferrocene groups in the organic links of the zirconia based **PEPEP-PIZOF-2** MOF,²⁹ and prepared MOF SSS thin-film electrodes to observe how the electron hopping between alkyl-ferrocene changes with varied ferrocene content. This was achieved by simply varying the ratios of redox-active and inactive links such as **Fc** and **NR** (**Fc** = alkyl-ferrocene containing link and **NR** = non-redox active link, Figure 1b), respectively, leading to observable changes in redox conductivity that resemble electrochemical behavior in solution. Cyclic voltammetry (CV) and potential-controlled chronocoulometry showed that the conductivity is diffusion controlled and is dependent on the **Fc** link content. Since the ferrocene RAMs are

covalently attached to the MOF, their long-range mobility is restricted, thus the diffusion-controlled conductivity arises solely from electron exchange between ferrocene pendants. The prepared MOF thin-film electrodes display the expected spectroelectrochemical response from the ferricenium/ferrocene pair. Experimentation of MOF films for over 1,000 CV cycles in aqueous sulfuric acid demonstrated their chemical, structural, and redox stability. Thus, the MOF-based SSS platform presented here is appropriate for fundamental charge transport studies and MOF-based devices.

Thin films of MOFs with formula $Zr_6O_4(OH)_4[Fc_xNR_{1-x}]_6$ containing varied SSS x input amounts of redox active linkers (Table S1) were grown onto fluorine-doped tin oxide (FTO) substrates via solvothermal synthesis in *N,N*-dimethylformamide (DMF) with $ZrOCl_2$ and benzoic acid for 48 h at 110 °C (Figure 1b). Treating the clean FTO substrates by immersing them in a **Fc** solution for 24 h before solvothermal growth ensured the formation of films with complete coverage and thicknesses between 5–7 μm , as determined by optical profilometry (Section S7). Scanning electron microscopy coupled with electron dispersive X-ray spectroscopy (SEM/EDXS) analysis of the films showed homogeneous distribution of octahedrally shaped crystallites with homogeneously dispersed Fe throughout the film. The Zr/Fe ratio measured from EDXS displayed a near 1:1 input/output incorporation of **Fc** links in the matrix (Figure 2a). Powder X-ray diffraction in grazing incidence mode (GIXD, Figure 2b) showed that the films are highly crystalline and isotropic, and exhibit sharp diffraction lines that were assigned to the MOF and FTO. High intensity peaks at low angle (4.08° 2-theta, $\text{CuK}\alpha$) confirmed the formation of the *Fd-3m* cubic phase of **PIZOF-2** throughout the series. The thin-film growing media also produced bulk powders that, after base digestion and ^1H NMR spectroscopy analysis, exhibited the same linker incorporation ratio as in the thin films. The bulk powders exhibit high porosity, with N_2 adsorption uptakes and Brunauer-Emmett-Teller (BET) surface areas consistent with increased alkyl-ferrocene loading (Table S6) between 1922–1331 $\text{m}^2 \text{g}^{-1}$. Interestingly, increasing **Fc** content also results in change in isotherm type from mesoporous in $x = 0$ mol%, to microporous in $x = 100$ mol% (Figure S24) as result of pore filling by the alkyl-ferrocene pendants. The MOF powders are also stable to humidity, retaining their crystallinity and BET surface area even after H_2O vapor adsorption cycles at 300 K (Section S9).

Cyclic voltammetry of the prepared MOF thin-film electrodes, (Figure 3a) shows a redox system undergoing linear diffusion. In contrast to surface-confined redox species with instantaneously accessible RAMs, which display symmetrical Gaussian-shaped peaks and a linear dependence of peak current with scan rate,³⁰ our MOFs display peak separation and square-root dependence on scan rate (Figure 3b), characteristic of a 1-dimensional diffusive system. We ascribe the larger peak splitting observed in these CVs compared to an ideal diffusive system, *i.e.*, 57 mV for a one-electron exchange, as the sum of resistances derived from the non-metallic character of the film. A fundamental difference between the behaviors of ferrocene dissolved in $Zr_6O_4(OH)_4[Fc_xNR_{1-x}]_6$ MOFs and a freely diffusing redox species in liquid solution is that the redox centers in the former are spatially fixed, restricting the charge migration mechanism to electron hopping between neighboring RAM sites. This condition allows for strong modulation of electron transport properties by means of redox center loading, which in our case is controlled *a priori* by the input ratios of **Fc**/**NR** linkers. Figure 3c shows the effects of **Fc** loading in the $Zr_6O_4(OH)_4[Fc_xNR_{1-x}]_6$ films on voltammetric peak currents displaying non-linear trends, in strong contrast to the linear dependence of peak current versus concentration in freely diffusive redox systems.³¹ UV-vis spectroscopy indicates that we can electrochemically oxidize a substantial amount of ferrocene within the films, implying charge can

travel from the FTO through the rest of the MOF. After 15 min of oxidative charging, films with high **Fc** content display a clear absorbance peak near 630 nm (Figure 4a), indicating a change from ferrocene to ferricenium ion. This absorbance peak coincides with a visible color change in the more concentrated films from orange-yellow (ferrocene) to bluish-green (ferricenium, Figure S8). Section S5 in the SI contains the UV-vis results of all the films.

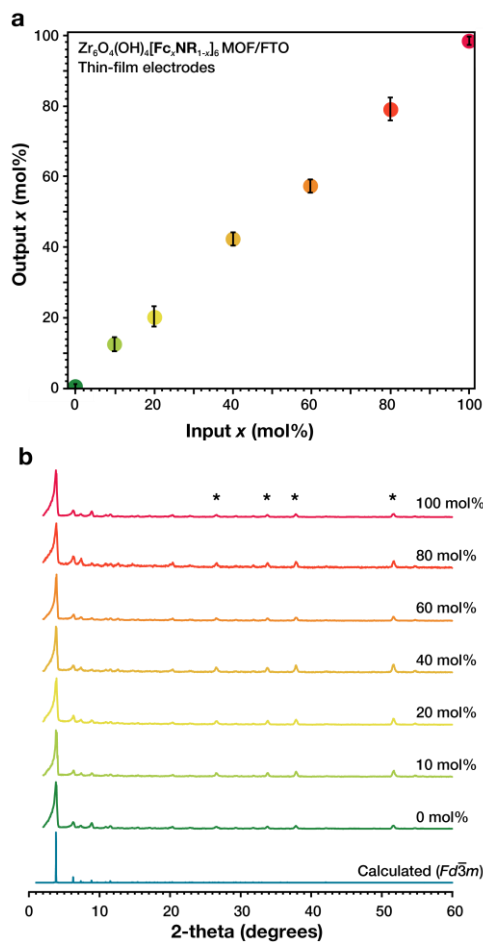


Figure 2. MOF film characterization. (a) Plot of the SSS input-output mol% ratio of the **Fc** link incorporated in the thin film MOFs as determined by EDXS, evidencing 1:1 input-output incorporation. (b) GIXD of MOF thin films grown on FTO substrates. Stars denote peaks corresponding to FTO.

Changes in redox hopping dynamics resulting from redox center dilution were probed by evaluating the diffusion coefficient of charge transfer (D_e). In our MOF, we expect the distance that electrons need to hop between sites to be higher for more dilute samples, causing D_e values to lower with decreasing **Fc** loading. To test this hypothesis, we measured diffusion coefficients of oxidative and reductive charging in the film through chronocoulometry by subsequent oxidizing and reducing potential steps. Anson plots,³¹ which graph charge collected versus square root of time, were used to extract diffusion coefficients (Figure S9). We used a model³² developed for redox-active polymeric films to predict theoretical diffusion coefficients of charge transfer as a function of concentration (Figure 4c). This model derives diffusion coefficients in redox pendant networks from charge transfer dynamics via the Dahms-Ruff expression^{33–35} with restricted physical diffusion of redox species (Eq. 1), and the exchange kinetics expression (Eq. 2):

$$D_e = \frac{1}{6} k_{et} r_{NN}^2 \quad (1)$$

$$k_{et} = k' e^{-(r_{NN}-r_0)/\delta} \quad (2)$$

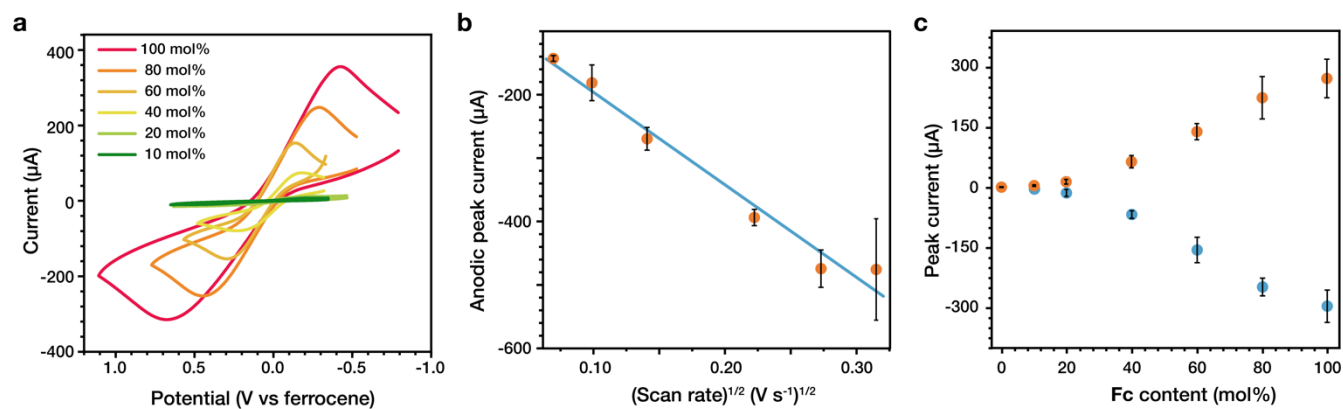


Figure 3. Cyclic voltammetry data of **Fc** containing MOF electrodes. (a) Cyclic voltammograms at various **Fc** link content (scan rate of 20 mV s⁻¹, in 0.1 M LiBF₄ in MeCN and Pt counter electrode). (b) Peak current of the 100% **Fc** MOF electrode as a function of the square root of scan rate. (c) Peak currents of the MOF electrodes as a function of their ferrocene content (scan rate of 20 mV s⁻¹).

where k_{et} is the electron self-exchange rate constant, and r_{NN} is the average distance between nearest neighboring pendants, k' is the intrinsic facility of charge transfer between pendants, δ is a characteristic length representing electronic coupling strength in the medium, and r_0 is the contact radius of the pendant (see p. S27-28 for details). The model predicts that D_e increases exponentially at low concentrations, eventually becoming roughly linear. Values for k' and δ were found by fitting the theoretical curve to the experimental data points. The k' value obtained, $1.2 \times 10^7 \text{ s}^{-1}$, is larger, but comparable to the rate observed on ferrocene anchored to a metal electrode ($k' = 1.6 \times 10^6 \text{ s}^{-1}$).³⁶ The δ value, 1.1 Å, is similar to the analogous distance-dependence constant for electron transfer through saturated alkane chains.³⁷⁻³⁸

The prediction that high pendant-pendant distance at low concentrations causes sluggish charge diffusion aligns with percolation theory, which applies to the conductivity of networks in which the nodes are a random distribution of conductors (pendants) and insulators (unmodified linkers). Percolation theory predicts that there is some critical ratio of conductors in a given network below which the network ceases to effectively conduct.³⁹ Indeed, the critical ratios for 3D networks related to our MOF (isotropic cubic lattice with 6-12 nearest neighbors) are in the range of 20-30 mol% **Fc**.⁴⁰ The redox conductivity of the MOFs was obtained from the Einstein-Stokes equation for charged diffusive systems, using the experimentally determined electron diffusion coefficients, resulting in composition-dependent redox conductivity with a maximum value of $\sigma_e = 1.10 \text{ mS m}^{-1}$ in the 100% **Fc** MOF (Figure 4c), comparable to the intrinsic electron conductivity of undoped silicon (1.56 mS m^{-1}).⁴¹

The structural and electrochemical stability of the prepared films was probed by exposing the 100 mol% **Fc** MOF electrode to multiple CV charge-discharge cycles in 0.1 M H₂SO₄(aq). After 1500 cycles (Figure 4d) the only observable change in the voltammogram is a slight shift in peak current over time, related to improved wetting of the electrolyte. GIXD of the cycled film showed very little changes in diffraction pattern (Figure S30), evidencing retention of the MOF architecture.

We have demonstrated a new metal-organic framework design with capabilities for fine-tuning of redox pendant concentration. This tunability was exploited to study the effect of redox pendant concentration on electroactivity. Our results imply there is a set of parameters that determine electrochemical accessibility in redox-modified MOF films:

pendant RAM concentration and self-exchange kinetics. Ongoing work in our laboratories centers on establishing the impact of these charge transfer dynamics on device performance and evaluating the interplay between redox properties and access to MOF porosity in functional films.

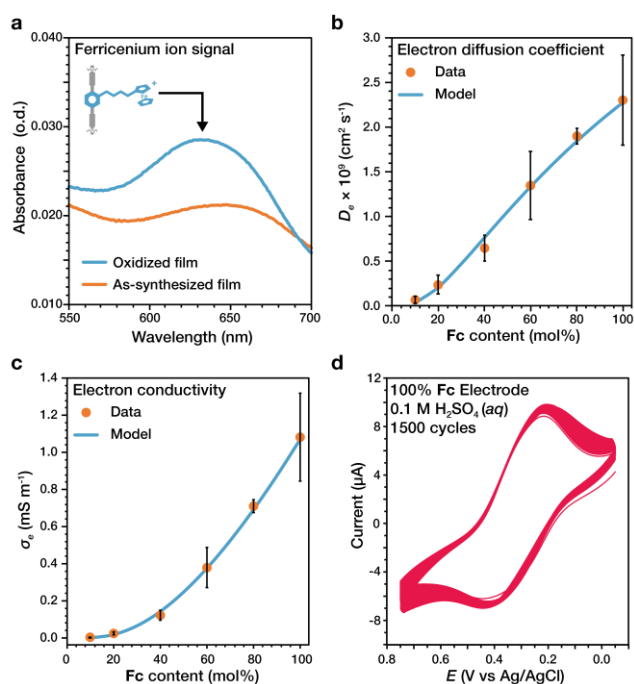


Figure 4. Charge transport in redox-active MOF films. (a) UV-visible absorption spectra of 100 mol% **Fc** MOF thin film before (orange trace) and after oxidation (blue trace), evidencing the formation of ferricenium ion. (b) Absorbance of ferricenium as a function of **Fc** content in the MOF thin films. (c) Diffusion coefficient of electron transfer derived from Anson plots as function of **Fc** content (orange symbols), compared to modeled D_e from Eqs. (1) and (2) (blue line). (d) Cyclic voltammetry of a 100% **Fc** electrode in 0.1 M H₂SO₄(aq) over 1500 cycles.

ASSOCIATED CONTENT

Supporting Information

The Supporting Information is available free of charge on the ACS Publications website.

Experimental procedures for linker synthesis, MOF thin-film and bulk crystallization, PXRD of bulk MOF powders, NMR/EDXS composition studies, SEM and optical microscopy images, electrochemical methods and modeling, gas adsorption isotherms, MOF stability analyses, TGA data, infrared spectroscopy, and $^1\text{H}/^{13}\text{C}$ NMR spectra.

AUTHOR INFORMATION

Corresponding Author

*fernando@ucf.edu

*joaquir@illinois.edu

Author Contributions

‡These authors contributed equally.

Notes

The authors declare no competing financial interests.

ACKNOWLEDGMENT

This research was carried out in part in the Materials Research Laboratory Central Facilities, University of Illinois and Materials Characterization Facility AMPAC, University of Central Florida. FJU-R and JRL acknowledge the Scallog Advanced Energy Storage Fellowship for enabling discussions leading to the conception of this work. JRL acknowledges the Alfred P. Sloan Foundation Fellowship.

REFERENCES

- Li, Y.; Pang, A.; Wang, C.; Wei, M., Metal-organic frameworks: promising materials for improving the open circuit voltage of dye-sensitized solar cells. *Journal of Materials Chemistry* **2011**, *21* (43), 17259-17264.
- Zhu, J.; Maza, W. A.; Morris, A. J., Light-harvesting and energy transfer in ruthenium(II)-polypyridyl doped zirconium(IV) metal-organic frameworks: A look toward solar cell applications. *Journal of Photochemistry and Photobiology A: Chemistry* **2017**, *344*, 64-77.
- Chueh, C.-C.; Chen, C.-I.; Su, Y.-A.; Konnerth, H.; Gu, Y.-J.; Kung, C.-W.; Wu, K. C. W., Harnessing MOF materials in photovoltaic devices: recent advances, challenges, and perspectives. *Journal of Materials Chemistry A* **2019**, *7* (29), 17079-17095.
- Xia, W.; Mahmood, A.; Zou, R.; Xu, Q., Metal-organic frameworks and their derived nanostructures for electrochemical energy storage and conversion. *Energy & Environmental Science* **2015**, *8* (7), 1837-1866.
- Xu, G.; Nie, P.; Dou, H.; Ding, B.; Li, L.; Zhang, X., Exploring metal organic frameworks for energy storage in batteries and supercapacitors. *Materials Today* **2017**, *20* (4), 191-209.
- Li, Y.; Xu, Y.; Yang, W.; Shen, W.; Xue, H.; Pang, H., MOF-Derived Metal Oxide Composites for Advanced Electrochemical Energy Storage. *Small* **2018**, *14* (25), 1704435.
- Liu, B.; Baumann, A. E.; Thoi, V. S., Modulating charge transport in MOFs with zirconium oxide nodes and redox-active linkers for lithium sulfur batteries. *Polyhedron* **2019**, *170*, 788-795.
- Downes, C. A.; Marinescu, S. C., Electrocatalytic Metal-Organic Frameworks for Energy Applications. *ChemSusChem* **2017**, *10* (22), 4374-4392.
- Johnson, B. A.; Bhunia, A.; Fei, H.; Cohen, S. M.; Ott, S., Development of a UiO-Type Thin Film Electrocatalysis Platform with Redox-Active Linkers. *Journal of the American Chemical Society* **2018**, *140* (8), 2985-2994.
- Yan, Y.; He, T.; Zhao, B.; Qi, K.; Liu, H.; Xia, B. Y., Metal/covalent-organic frameworks-based electrocatalysts for water splitting. *Journal of Materials Chemistry A* **2018**, *6* (33), 15905-15926.
- Kung, C.-W.; Chang, T.-H.; Chou, L.-Y.; Hupp, J. T.; Farha, O. K.; Ho, K.-C., Porphyrin-based metal-organic framework thin films for electrochemical nitrite detection. *Electrochemistry Communications* **2015**, *58*, 51-56.

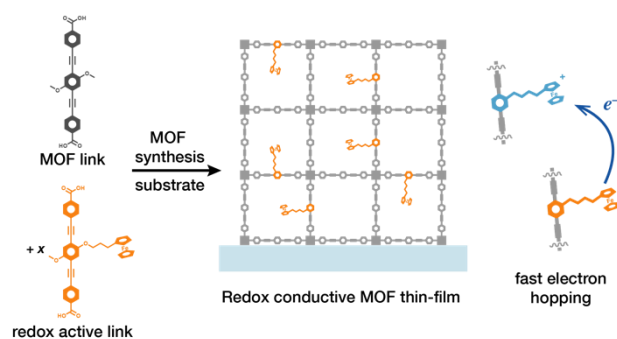
- Chen, J.; Yu, C.; Zhao, Y.; Niu, Y.; Zhang, L.; Yu, Y.; Wu, J.; He, J., A novel non-invasive detection method for the FGFR3 gene mutation in maternal plasma for a fetal achondroplasia diagnosis based on signal amplification by hemin-MOFs/PtNPs. *Biosensors and Bioelectronics* **2017**, *91*, 892-899.
- Wang, X.; Yang, C.; Zhu, S.; Yan, M.; Ge, S.; Yu, J., 3D origami electrochemical device for sensitive Pb^{2+} testing based on DNA functionalized iron-porphyrinic metal-organic framework. *Biosensors and Bioelectronics* **2017**, *87*, 108-115.
- Kempahanumakkagari, S.; Vellingiri, K.; Deep, A.; Kwon, E. E.; Bolan, N.; Kim, K.-H., Metal-organic framework composites as electrocatalysts for electrochemical sensing applications. *Coordination Chemistry Reviews* **2018**, *357*, 105-129.
- Talin, A. A.; Centrone, A.; Ford, A. C.; Foster, M. E.; Stavila, V.; Haney, P.; Kinney, R. A.; Szalai, V.; El Gabaly, F.; Yoon, H. P.; Léonard, F.; Allendorf, M. D., Tunable Electrical Conductivity in Metal-Organic Framework Thin-Film Devices. *Science* **2014**, *343* (6166), 66-69.
- Hod, I.; Bury, W.; Gardner, D. M.; Deria, P.; Roznyatovskiy, V.; Wasielewski, M. R.; Farha, O. K.; Hupp, J. T., Bias-Switchable Permselectivity and Redox Catalytic Activity of a Ferrocene-Functionalized, Thin-Film Metal-Organic Framework Compound. *The Journal of Physical Chemistry Letters* **2015**, *6* (4), 586-591.
- Liu, J.; Wächter, T.; Irmeler, A.; Weidler, P. G.; Gliemann, H.; Pauly, F.; Mugnaini, V.; Zharnikov, M.; Wöll, C., Electric Transport Properties of Surface-Anchored Metal-Organic Frameworks and the Effect of Ferrocene Loading. *ACS Applied Materials & Interfaces* **2015**, *7* (18), 9824-9830.
- Chen, Q.; Sun, J.; Li, P.; Hod, I.; Moghadam, P. Z.; Kean, Z. S.; Snurr, R. Q.; Hupp, J. T.; Farha, O. K.; Stoddart, J. F., A Redox-Active Bistable Molecular Switch Mounted inside a Metal-Organic Framework. *Journal of the American Chemical Society* **2016**, *138* (43), 14242-14245.
- Hod, I.; Farha, O. K.; Hupp, J. T., Modulating the rate of charge transport in a metal-organic framework thin film using host:guest chemistry. *Chemical Communications* **2016**, *52* (8), 1705-1708.
- Wang, T. C.; Hod, I.; Audu, C. O.; Vermeulen, N. A.; Nguyen, S. T.; Farha, O. K.; Hupp, J. T., Rendering High Surface Area, Mesoporous Metal-Organic Frameworks Electronically Conductive. *ACS Applied Materials & Interfaces* **2017**, *9* (14), 12584-12591.
- Palmer, R. H.; Liu, J.; Kung, C.-W.; Hod, I.; Farha, O. K.; Hupp, J. T., Electroactive Ferrocene at or near the Surface of Metal-Organic Framework UiO-66. *Langmuir* **2018**, *34* (16), 4707-4714.
- Celis-Salazar, P. J.; Cai, M.; Cucinell, C. A.; Ahrenholtz, S. R.; Epley, C. C.; Usov, P. M.; Morris, A. J., Independent Quantification of Electron and Ion Diffusion in Metallocene-Doped Metal-Organic Frameworks Thin Films. *Journal of the American Chemical Society* **2019**, *141* (30), 11947-11953.
- Nelsen, S. F.; Trieber, D. A.; Nagy, M. A.; Konradsson, A.; Halfen, D. T.; Splan, K. A.; Pladzewicz, J. R., Structural Effects on Intermolecular Electron Transfer Reactivity. *Journal of the American Chemical Society* **2000**, *122* (25), 5940-5946.
- Hu, L.; Zhai, T.; Li, H.; Wang, Y., Redox-Mediator-Enhanced Electrochemical Capacitors: Recent Advances and Future Perspectives. *ChemSusChem* **2019**, *12* (6), 1118-1132.
- Landa-Medrano, I.; Lozano, I.; Ortiz-Vitoriano, N.; Ruiz de Larramendi, I.; Rojo, T., Redox mediators: a shuttle to efficacy in metal- O_2 batteries. *Journal of Materials Chemistry A* **2019**, *7* (15), 8746-8764.
- Singh, V.; Kim, S.; Kang, J.; Byon, H. R., Aqueous organic redox flow batteries. *Nano Research* **2019**, *12* (9), 1988-2001.
- Deng, H.; Doonan, C. J.; Furukawa, H.; Ferreira, R. B.; Towne, J.; Knobler, C. B.; Wang, B.; Yaghi, O. M., Multiple Functional Groups of Varying Ratios in Metal-Organic Frameworks. *Science* **2010**, *327* (5967), 846-850.
- Newsome, W. J.; Ayad, S.; Cordova, J.; Reinheimer, E. W.; Campiglia, A. D.; Harper, J. K.; Hanson, K.; Uribe-Romo, F. J., Solid State Multicolor Emission in Substitutional Solid Solutions of Metal-Organic Frameworks. *J. Am. Chem. Soc.* **2019**, *141* (28), 11298-11303.
- Schaate, A.; Roy, P.; Preuß, T.; Lohmeier, S. J.; Godt, A.; Behrens, P., Porous Interpenetrated Zirconium-Organic Frameworks (PIZOFs): A Chemically Versatile Family of Metal-Organic Frameworks. *Chemistry - A European Journal* **2011**, *17* (34), 9320-9325.
- Laviron, E., General Expression of the Linear Potential Sweep Voltammogram in the case of Diffusionless Electrochemical Systems. *J. Electroanal. Chem.* **1979**, *101*, 19-28.

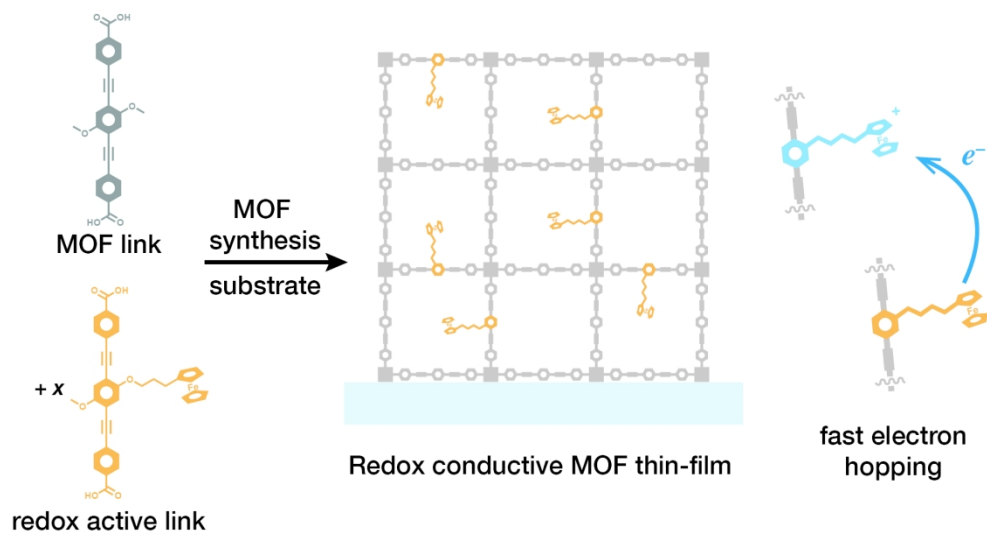
- 1
2
3
4
5
6
7
8
9
10
11
12
13
14
15
16
17
18
19
20
21
22
23
24
25
26
27
28
29
30
31
32
33
34
35
36
37
38
39
40
41
42
43
44
45
46
47
48
49
50
51
52
53
54
55
56
57
58
59
60
31. Bard, A. J.; Faulkner, L. R., *Electrochemical Methods: Fundamentals and Applications*, 2nd ed. John Wiley & Sons, Inc.: 2001.
32. Fritsch-Faules, I.; Faulkner, L. R., A Microscopic Model for Diffusion of Electrons by Successive Hopping among Redox Centers in Networks. *J. Electroanal. Chem.* **1989**, 263, 237-255.
33. Ruff, I.; Friedrich, V. J., Transfer Diffusion I. Theoretical. *J. Phys. Chem.* **1971**, 75 (21), 3297-3302.
34. Ruff, I.; Friedrich, V. J.; Demeter, K.; Csillag, K., Transfer Diffusion II. Kinetics of Electron Exchange Reaction between Ferrocene and Ferricinium Ion in Alcohols. *J. Phys. Chem.* **1971**, 75 (21), 3303-3309.
35. Dahms, H., Electronic Conduction in Aqueous Solution. *J. Phys. Chem.* **1968**, 72 (1), 362-364.
36. Smalley, J. F.; Feldberg, S. W.; Chidsey, C. E. D.; Linford, M. R.; Newton, M. D.; Liu, Y.-P., The Kinetics of Electron Transfer through Ferrocene-Terminated Alkanethiol Monolayers on Gold. *J. Phys. Chem.* **1995**, 99, 13141-13149.
37. Smalley, J. F.; Finklea, H. O.; Chidsey, C. E. D.; Linford, M. R.; Creager, S. E.; Ferraris, J. P.; Chalfant, K.; Zawodzinski, T.; Feldberg, S. W.; Newton, M. D., Heterogeneous Electron-Transfer Kinetics for Ruthenium and Ferrocene Redox Moieties through Alkanethiol Monolayers on Gold. *J. Am. Chem. Soc.* **2003**, 125, 2004-2013.
38. Johnson, M. D.; Miller, J. R.; Green, N. S.; Closs, G. L., Distance Dependence of Intramolecular Hole and Electron Transfer in Organic Radical Ions. *J. Phys. Chem.* **1989**, 93 (4), 1173-1176.
39. Stauffer, D.; Aharony, A., *Introduction to Percolation Theory*. Taylor & Francis Inc.: Philadelphia, PA, 2010.
40. Tran, J.; Yoo, T.; Stahlheber, S.; Small, A., Percolation Thresholds on Three-Dimensional Lattices with Three Nearest Neighbors. *J. Stat. Mech.* **2013**, P05014.
41. Serway, R. A., *Principles of Physics*. 2nd ed.; Saunders College Publishing: Fort Worth, TX, 1998.

1
2
3
4
5
6
7
8
9
10
11
12
13
14
15
16
17
18
19
20
21
22
23
24
25
26
27
28
29
30
31
32
33
34
35
36
37
38
39
40
41
42
43
44
45
46
47
48
49
50
51
52
53
54
55
56
57
58
59
60

Authors are required to submit a graphic entry for the Table of Contents (TOC) that, in conjunction with the manuscript title, should give the reader a representative idea of one of the following: A key structure, reaction, equation, concept, or theorem, etc., that is discussed in the manuscript. Consult the journal's Instructions for Authors for TOC graphic specifications.

Insert Table of Contents artwork here





165x89mm (300 x 300 DPI)

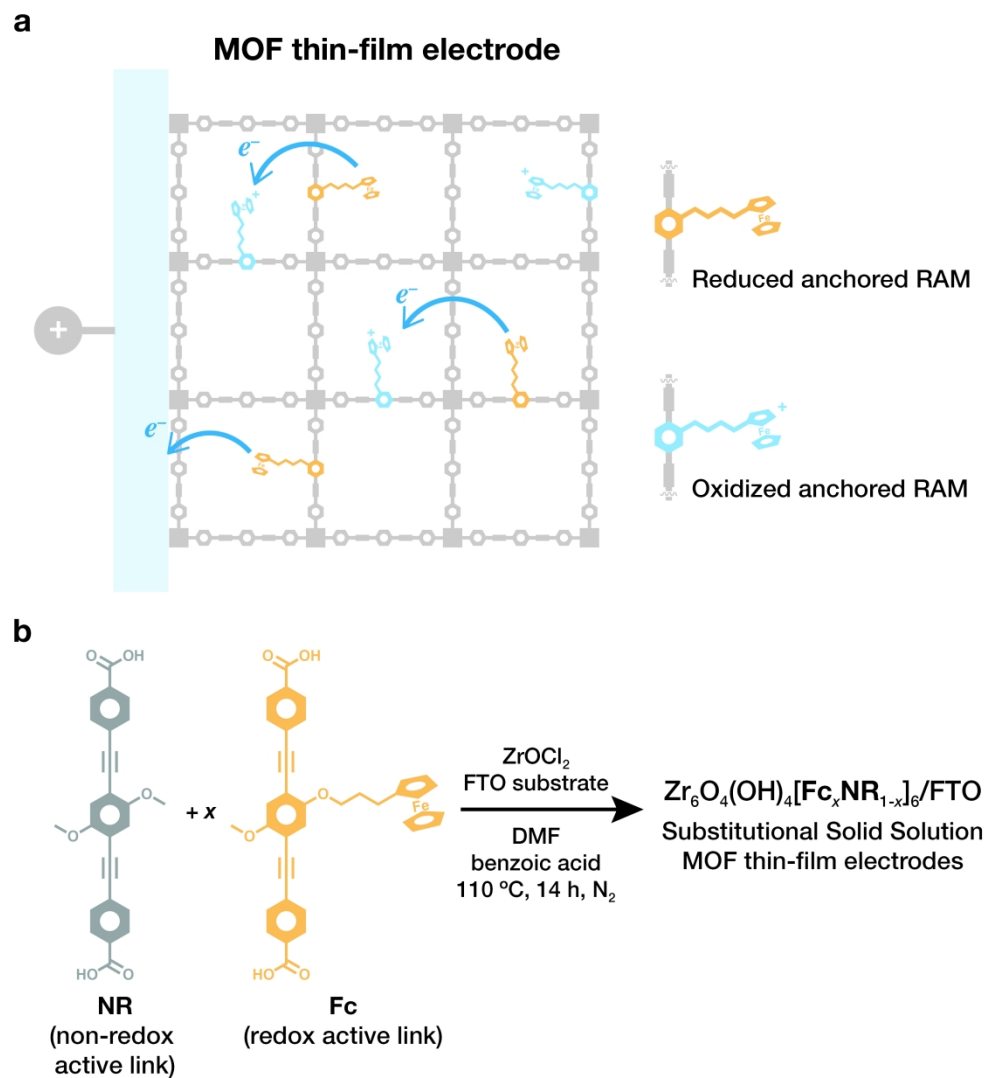
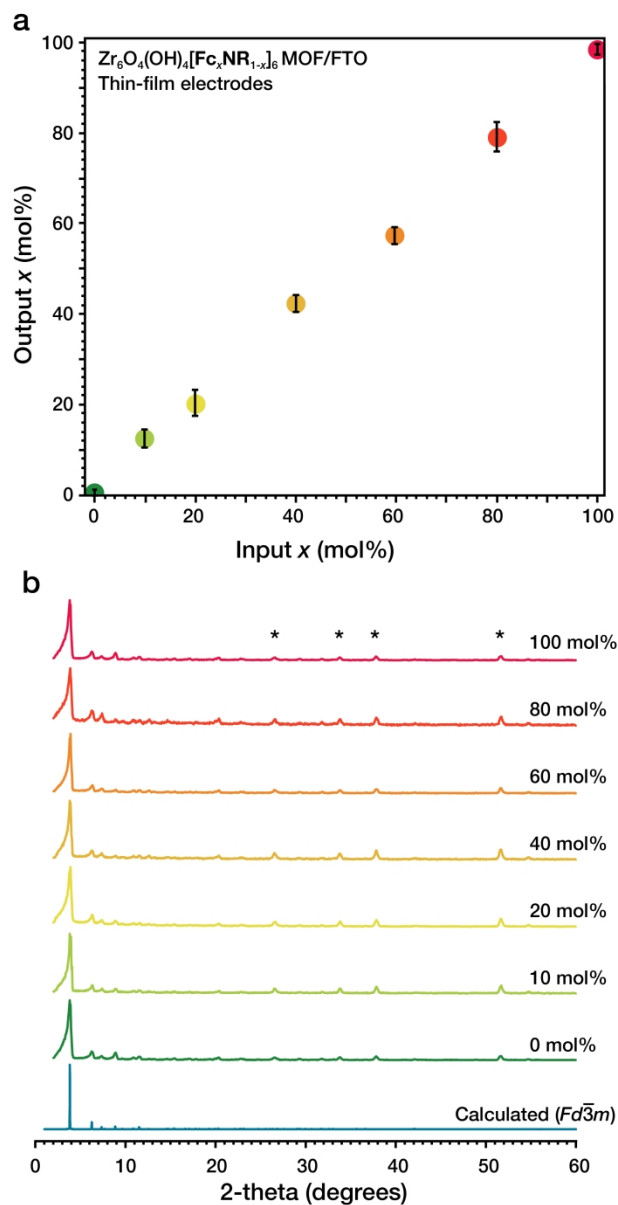


Figure 1. (a) Depiction of a MOF thin film electrode containing varied amounts of redox active links that enable fast redox conductivity via redox hopping. (b) Synthesis of MOF thin film electrodes with finely tunes substitutional solid solution amounts of redox active links.

286x309mm (300 x 300 DPI)



45 Figure 2. MOF film characterization. (a) Plot of the SSS input-output mol% ratio of the Fc link incorporated
46 in the thin film MOFs as determined by EDXS, evidencing 1:1 input-output incorporation. (b) GIXD of MOF
47 thin films grown on FTO substrates. Stars denote peaks corresponding to FTO.

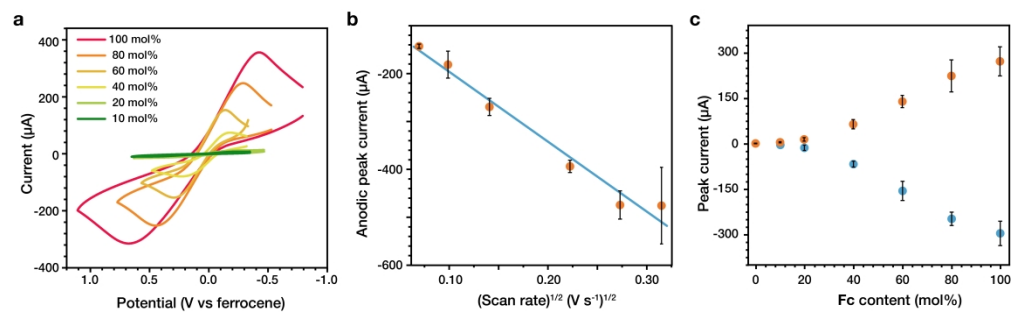


Figure 3. Cyclic voltammetry data of Fc containing MOF electrodes. (a) Cyclic voltammograms at various Fc link content (scan rate of 20 mV s⁻¹, in 0.1 M LiBF₄ in MeCN and Pt counter electrode). (b) Peak current of the 100% Fc MOF electrode as a function of the square root of scan rate. (c) Peak currents of the MOF electrodes as a function of their ferrocene content (scan rate of 20 mV s⁻¹).

625x189mm (300 x 300 DPI)

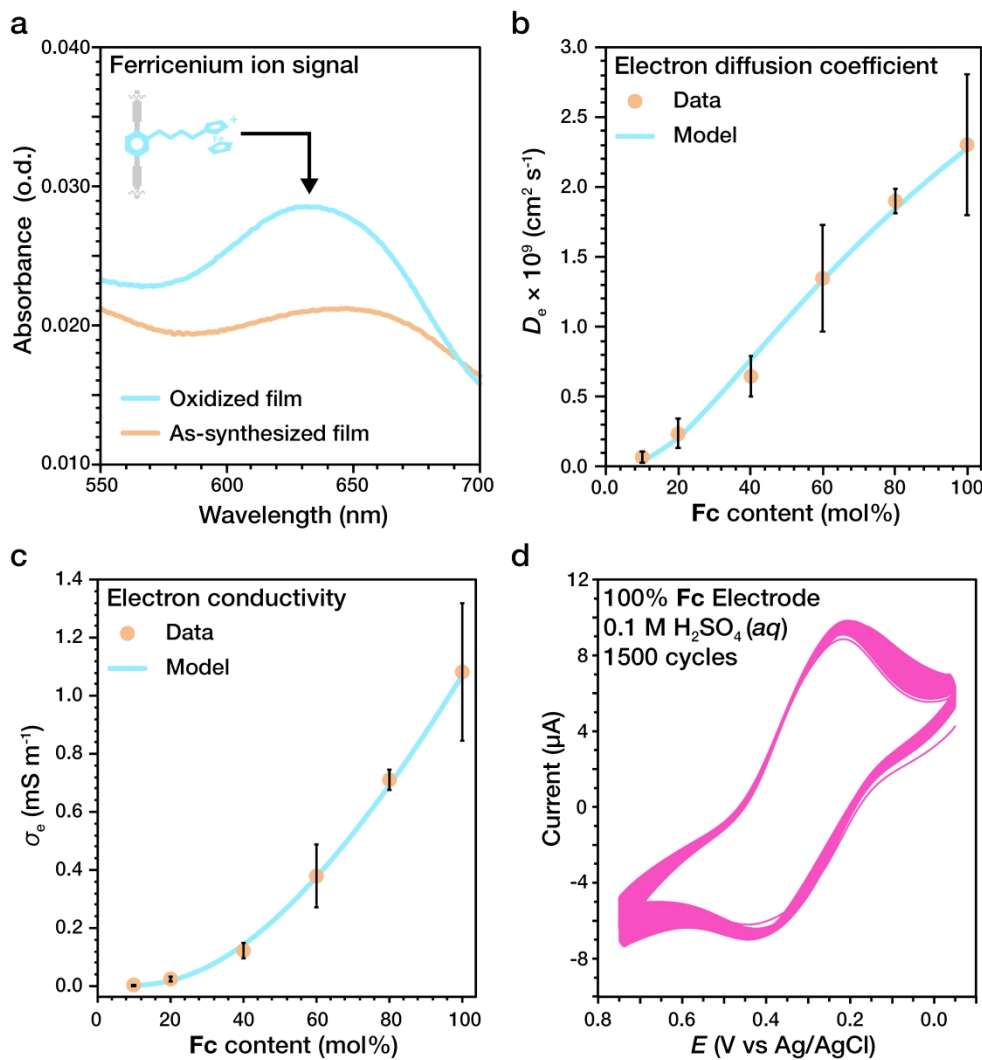


Figure 4. Charge transport in redox-active MOF films. (a) UV-visible absorption spectra of 100 mol% Fc MOF thin film before (orange trace) and after oxidation (blue trace), evidencing the formation of ferricenium ion. (b) Absorbance of ferricenium as a function of Fc content in the MOF thin films. (c) Diffusion coefficient of electron transfer derived from Anson plots as function of Fc content (orange symbols), compared to modeled D_e from Eqs. (1) and (2) (blue line). (d) Cyclic voltammetry of a 100% Fc electrode in 0.1 M H₂SO₄ (aq) over 1500 cycles.